Available online at www.sciencedirect.com
SCIENCE DIRECT®
Physica D 186 (2003) 69–92
PHYSICA D
www.elsevier.com/locate/physd

Polarization switching of light interacting with a degenerate two-level optical medium

Julie A. Byrne [a], Ildar R. Gabitov [b], Gregor Kovačič [c,*]

[a] *Mathematics Department, Siena College, 515 Loudon Road, Loudonville, NY 12211-1462, USA*
[b] *Mathematics Department, University of Arizona, 617 North Santa Rita, P.O. Box 210089, Tucson, AZ 85721, USA*
[c] *Mathematical Sciences Department, Rensselaer Polytechnic Institute, Troy, NY 12180, USA*

Received 12 December 2002; received in revised form 9 June 2003; accepted 25 June 2003
Communicated by C.K.R.T. Jones

Abstract

Polarization switching of light in a degenerate two-level medium, known as the Λ-configuration, is described. The polarization dynamics of light pulses is investigated by means of the inverse-scattering transform. The mathematical formalism of the inverse-scattering transform that takes into account the initial fluctuations of the medium polarization components corresponding to atomic transitions between the excited state and the two degenerate ground sub-levels in Λ-configuration atomic system is formulated. The characteristic switching length is evaluated via the physical parameters of the prepared medium and the optical pulse.

Keywords: Polarization switching; Degenerate two-level medium; Maxwell–Bloch equations; Solitons

1. Introduction

One of the simplest examples of resonant interaction between intense polarized light and a lossless active optical medium involves the Λ-configuration two-level medium, that is, a two-level medium with a degenerate ground level. In such a medium, the excited level has no angular momentum, corresponding to the quantum number $\ell = 0$. The ground sub-levels are part of a degenerate triplet lying on the same energy shell. All three have equal quantum number for the magnitude of the angular momentum, $\ell = 1$, but differ in the values of the quantum number for the vertical component of the angular momentum $m_\ell = 0, \pm 1$. In a relatively weak static magnetic field, the sub-levels forming the triplet split. Electronic transitions are permitted between the excited $\ell = 0$ state and each of the ground states $\ell = 1$, $m_\ell = \pm 1$ [1]. During these two transitions, the angular momentum m_ℓ changes by $+1$ or -1, respectively. By the conservation of angular momentum, the photons emitted in these transitions must have spin -1 and $+1$, respectively. Thus, in particular, the transition $|\ell = 0\rangle \leftrightarrow |\ell = 1, m_\ell = +1\rangle$ involves right-circularly polarized light, and the transition $|\ell = 0\rangle \leftrightarrow |\ell = 1, m_\ell = -1\rangle$ involves left-circularly polarized light. The quantum diagram for the two allowed transitions, shown in Fig. 1, resembles the capital Greek letter Λ, whence the name Λ-configuration.

* Corresponding author.
E-mail address: kovacg@rpi.edu (G. Kovačič).

0167-2789/$ – see front matter © 2003 Elsevier B.V. All rights reserved.
doi:10.1016/S0167-2789(03)00245-8

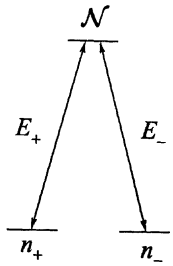

Fig. 1. Quantum diagram for the Λ-configuration transition.

This paper focuses on polarization switching in a Λ-configuration medium. In particular, if a light pulse is injected into a Λ-configuration medium with no initial material polarizabilities and population of the excited level, and if one of the two degenerate ground sub-levels is consistently more populated than the other, the polarization of the light pulse will switch in such a way that the pulse will interact only with the excited level and the less populated ground sub-level. Thus, deep into the medium, the electric field will be switched to purely circularly polarized, and the medium will undergo a pure two-level transition. As a result, we propose a very simple mechanism for a polarization switch: a degenerate two-level Λ-configuration medium, with no initial material polarizability, and with only one ground sub-level occupied. Arbitrarily polarized light impinging on this medium will switch all its polarization into circular polarization, whose handedness will depend on which ground sub-level is excited. We would like to point out that this switching is in stark contrast with the usual linear polarizers, which simply discard the unwanted polarization component. In a Λ-configuration medium, the energy is retained in the nonlinear process of polarization switching through the resonant interaction between the light pulse and the medium.

We have found our result by utilizing the inverse-scattering transform method [2–10]. For pulse propagation in two-level resonant media, this method was first used in [11], where the Lax-pair of the problem was discovered, after strong evidence of integrability including an infinite number of conserved quantities and a wealth of exact solutions had been given in [12,13]. A comprehensive theory of the two-level problem based on the inverse-scattering transform was developed in [11,14–21]. In [22–36], the inverse-scattering transform and related methods were used to find large classes of solutions for the degenerate two-level media and certain three-level media. A comprehensive review of the inverse-scattering transform technique for multi-level systems is presented in [37].

The rest of the paper is organized as follows. In Section 2, we describe the Λ-configuration Maxwell–Bloch equations and their simplest properties and solutions. In Section 3, we use the inverse-scattering transform method to show the polarization-switching property in general, and illustrate it on several cases of one- and multi-soliton solutions. We also show how to obtain almost complete polarization conversion from one circular component to the opposite component by controlling the initial populations of the two degenerate ground sub-levels, and discuss physical parameters needed to produce this conversion in practice. In Section 4, we discuss the details of the polarization dynamics exhibited by the one- and multi-soliton solutions of the Λ-configuration Maxwell–Bloch equations at any given point in space and time. Finally, in Section 5, we present a brief set of conclusions.

2. The Maxwell–Bloch equations

Resonant propagation of intense light through a Λ-configuration two-level active optical medium with a degenerate ground level is described by the following set of Maxwell–Bloch equations:

$$\frac{\partial E_\pm}{\partial x} = \int_{-\infty}^{\infty} \rho_\pm g(\lambda)\,\mathrm{d}\lambda, \tag{1a}$$

$$\frac{\partial \rho_+}{\partial t} - 2\mathrm{i}\lambda\rho_+ = \frac{1}{2}[E_+(\mathcal{N} - n_+) - E_-\mu^*], \tag{1b}$$

$$\frac{\partial \rho_-}{\partial t} - 2\mathrm{i}\lambda\rho_- = \frac{1}{2}[E_-(\mathcal{N} - n_-) - E_+\mu], \tag{1c}$$

$$\frac{\partial \mathcal{N}}{\partial t} = -\frac{1}{2}[E_+\rho_+^* + E_+^*\rho_+ + E_-\rho_-^* + E_-^*\rho_-], \tag{1d}$$

$$\frac{\partial n_\pm}{\partial t} = \frac{1}{2}[E_\pm\rho_\pm^* + E_\pm^*\rho_\pm], \tag{1e}$$

$$\frac{\partial \mu}{\partial t} = \frac{1}{2}[E_+^*\rho_- + E_-\rho_+^*]. \tag{1f}$$

In these equations, the subscripts $+$ and $-$ refer to the two degenerate ground sub-levels with quantum projections of the angular momentum equal to $m_\ell = 1$ and $m_\ell = -1$, respectively. The complex-valued electric field envelopes $E_\pm(x, t)$ represent the components of the electric field that take part in the transitions between each of the respective sub-levels and the excited level. The corresponding complex-valued material polarizability envelopes are described by the functions $\rho_\pm(x, t, \lambda)$. The parameter λ represents the detuning from the exact quantum transition frequency due to the Doppler shift, which is caused by the thermal motion of the atoms in the medium. The velocities of these atoms are distributed according to the "inhomogeneous broadening" function $g(\lambda)$, which is non-negative and satisfies the equation $\int_{-\infty}^{\infty} g(\lambda)\,\mathrm{d}\lambda = 1$. The complex-valued function $\mu(x, t, \lambda)$ represents the polarizability envelope in the two-photon process that corresponds to the forbidden transition between the two degenerate ground sub-levels. The real-valued functions $n_\pm(x, t, \lambda)$ and $\mathcal{N}(x, t, \lambda)$ describe the population densities of the degenerate ground sub-levels and the excited level, respectively.

Eq. (1) are given in the light-cone coordinate frame, that is, the frame that is moving to the right with the speed of light. The coordinate change between this frame and the stationary laboratory frame is achieved by the transformation:

$$t = T - X, \qquad x = X, \tag{2}$$

where X and T represent the coordinates in the laboratory frame.

System (1) can also be written in the matrix form:

$$\frac{\partial H}{\partial x} = \frac{1}{4}\int_{-\infty}^{\infty} [J, \hat{\rho}]g(\lambda)\,\mathrm{d}\lambda, \tag{3a}$$

$$\frac{\partial \hat{\rho}}{\partial t} = [-H + \mathrm{i}\lambda J, \hat{\rho}] \tag{3b}$$

with

$$H = \frac{1}{2}\begin{bmatrix} 0 & E_+ & E_- \\ -E_+^* & 0 & 0 \\ -E_-^* & 0 & 0 \end{bmatrix}, \qquad \hat{\rho} = \begin{bmatrix} \mathcal{N} & \rho_+ & \rho_- \\ \rho_+^* & n_+ & \mu \\ \rho_-^* & \mu^* & n_- \end{bmatrix}, \qquad J = \begin{bmatrix} 1 & 0 & 0 \\ 0 & -1 & 0 \\ 0 & 0 & -1 \end{bmatrix} \tag{4}$$

and where $[A, B] = AB - BA$ is the commutator of the matrices A and B.

The Λ-configuration Maxwell–Bloch equations (1) are completely integrable. In particular, as shown in [23,24], these equations can be written in the 3×3 matrix Lax-pair form:

$$\frac{\partial \Phi}{\partial t} = U\Phi = (\mathrm{i}\lambda J - H)\Phi, \tag{5a}$$

$$\frac{\partial \Phi}{\partial x} = V\Phi = \frac{\mathrm{i}}{4}\left(\mathcal{P}\int_{-\infty}^{\infty}\frac{\hat{\rho}(x,t,\nu)}{\nu-\lambda}g(\nu)\,\mathrm{d}\nu\right)\Phi, \tag{5b}$$

where $\mathcal{P}$ stands for the Cauchy principal value of the integral, and H, $\hat{\rho}$, and J are defined in formula (4). The 3×3 matrix Φ is a simultaneous wave-function solution of both Eqs. (5a) and (5b). In order that these equations be compatible, that is, the mixed second derivatives of Φ be equal, Eqs. (3), and hence (1), must hold.

The boundary conditions corresponding to Eqs. (1) that we study in this paper are those of the signaling problem, which describe pulse propagation through a semi-infinite medium. In the most general version of this problem, input electric fields $E_{\pm}(0,t)$ are given at the entrance into the medium at $x=0$, and the limiting behavior of the material polarizabilities and population densities is given in the distant past as $t\to-\infty$. In particular, the limits:

$$\lim_{t\to-\infty}\mathcal{N}(x,t,\lambda), \qquad \lim_{t\to-\infty}n_{+}(x,t,\lambda), \qquad \lim_{t\to-\infty}n_{-}(x,t,\lambda), \qquad \lim_{t\to-\infty}\mu(x,t,\lambda)$$

are given as functions of x and λ, as are the functions $R_{\pm}(x,\lambda)$ in the asymptotic expressions:

$$\rho_{\pm}(x,t,\lambda)\sim \mathrm{e}^{2\mathrm{i}\lambda t}R_{\pm}^{*}(x,\lambda) \quad \text{as } t\to-\infty. \tag{6}$$

The validity of these last asymptotic expressions in not obvious, but follows from the derivation of the general inverse-scattering transform method for the Maxwell–Bloch equations. For non-degenerate two-level systems, this method was developed in [21]; it can be easily extended to the Λ and V-configurations. (The V-configuration is the "inverted" version of the Λ-configuration: the excited level contains two active degenerate sub-levels, while the ground level is non-degenerate.) This extension will be presented in a subsequent publication. In this paper, we assume

$$\lim_{t\to-\infty}\mu(x,t,\lambda)=0 \quad \text{and} \quad R_{\pm}(x,\lambda)=0, \tag{7}$$

where $R_{\pm}(x,\lambda)$ are defined in formula (6). Since we are interested in pulse-like solutions, we also require that $E_{\pm}(x,t)\to 0$ sufficiently rapidly for all x.

There exist several simple explicit solutions and special subsystems of the Λ-configuration Maxwell–Bloch system (1) that we describe here. The simplest solutions are stationary, with $E_{\pm}=0$, $\rho_{\pm}=0$, and $\mathcal{N}$, $n_{\pm}$, and μ arbitrary functions of x and λ.

Another special class of solutions includes inversionless waves. For this class, $\mathcal{N}(x,\lambda)=n_{+}(x,\lambda)=n_{-}(x,\lambda)$ is an arbitrary function of x and λ, $\mu(x,\lambda)=\rho_{\pm}(x,\lambda)=0$, and $E_{\pm}(x,t)=E_{\pm}(t)$, arbitrary functions of time t. Since all three atomic levels are equally occupied, the electric field propagates through the medium as if it were vacuum, at the speed of light, without disturbing the medium.

There exist two special, two-level sub-systems of the Λ-configuration Maxwell–Bloch system (1), obtained by setting either $E_{+}=\rho_{+}=n_{+}=\mu=0$ or $E_{-}=\rho_{-}=n_{-}=\mu=0$. These correspond to pure two-level transitions between the excited level and the $-$ or $+$ sub-levels, respectively. The inverse-scattering approach to two-level systems has been studied extensively in [11,14–21]. Of course, each of these sub-systems has its own stationary solutions and inversionless waves. As we show in Section 3.2, for a large class of physical initial conditions for which one ground sub-level is consistently more occupied than the other, the two-level transition corresponding to the more occupied sub-level is unstable, and the one corresponding to the less occupied sub-level is attracting. Thus, asymptotically for large x, the light-medium interaction evolves into the interaction of only one circularly polarized electric field component with a simple two-level medium.

From Eq. (3b), we can find three time-independent constraints of the Λ-configuration system (1), which are the respective traces of the matrices $\hat{\rho}$, $\hat{\rho}^2$, and $\hat{\rho}^3$. This is because the matrices $\hat{\rho}^2$ and $\hat{\rho}^3$ satisfy Eq. (3b) together with $\hat{\rho}$, and because the trace of any commutator vanishes identically. Explicitly, these quantities are

$$I_1(x,\lambda)=\mathcal{N}+n_{+}+n_{-},$$

$$I_2(x,\lambda) = \mathcal{N}^2 + n_+^2 + n_-^2 + 2(|\rho_+|^2 + |\rho_-|^2 + |\mu|^2)$$

and

$$I_3(x,\lambda) = \mathcal{N}^3 + n_+^3 + n_-^3 + 3[\mathcal{N}(|\rho_+|^2 + |\rho_-|^2) + n_+(|\rho_+|^2 + |\mu|^2) + n_-(|\rho_-|^2 + |\mu|^2) + \rho_+\rho_-^*\mu + \rho_+^*\rho_-\mu^*].$$

The first two of these correspond to the conservation of particles and unitarity, respectively.

3. Description of switching obtained via the inverse-scattering transform

In this section, we use the inverse-scattering transform method to describe the mechanism responsible for polarization switching in the Λ-configuration Maxwell–Bloch system (1) with initial conditions (7). Essentially, this switching is due to the uneven exponential evolution of the two spectral data components that roughly correspond to the two atomic transitions. More precisely, we will reveal the switching mechanism in two steps. First, we will demonstrate it for the N-soliton solutions. Then, we will use the fact that continuous radiation decays with increasing x to demonstrate this property for a large general class of optical pulses and pulse trains.

3.1. Review of direct and inverse-scattering

In this section, we briefly review the inverse-scattering transform method used to solve the general signaling problem for the Λ-configuration Maxwell–Bloch system (1). Let us recall that their Lax-pair is given by Eqs. (5), with the appropriate terms defined in formulas (4). Eqs. (5) form an over-determined system of ordinary differential equations for the wave-function Φ and the spectral parameter λ. We recall that since we are interested in pulse-like solutions, we require that $E_\pm(x,t) \to 0$ sufficiently rapidly as $t \to \pm\infty$ for all x.

The scattering problem for Eq. (5a) falls in the category of Manakov's problems [37–39]. We recall the Jost functions $\phi^\pm(x,t,\lambda)$ to be the solutions of Eq. (5a) that satisfy the asymptotic properties:

$$\phi^+(x, t\to\infty, \lambda) \sim \mathrm{e}^{\mathrm{i}\lambda Jt}, \qquad \phi^-(x, t\to-\infty, \lambda) \sim \mathrm{e}^{\mathrm{i}\lambda Jt}. \tag{8}$$

The Jost functions are related by the formula:

$$\phi^+(x,t,\lambda) = \phi^-(x,t,\lambda)S(x,\lambda) \tag{9}$$

for all real λ, with $S(x,\lambda)$ being the scattering matrix. Moreover, for real λ, the scattering matrix $S(x,\lambda)$ is unitary and $\det S(x,\lambda) = 1$. The matrix element $S_{11}(x,\lambda)$ can be analytically continued to the half-plane $\mathrm{Im}(\lambda) > 0$, and $S_{ij}(x,\lambda)$, $i,j = 2,3$, can be analytically continued to the half-plane $\mathrm{Im}(\lambda) < 0$. If the electric fields $E_\pm(x,t)$ decay as $\mathrm{e}^{-\gamma|t|}$ for some positive constant γ as $t \to \pm\infty$, these regions of analyticity can be extended to $\mathrm{Im}(\lambda) > -\gamma$ and $\mathrm{Im}(\lambda) < \gamma$, respectively.

The real values of λ form the continuous spectrum of Eq. (5a), and the zeros of $S_{11}(x,\lambda)$ in $\mathrm{Im}(\lambda) > 0$ give all the relevant eigenvalues of (5a). If $E(x,t) \to 0$ sufficiently rapidly as $t \to \pm\infty$, there is only a finite number, N, of these eigenvalues at $\lambda = \lambda_n$, $n = 1,\ldots,N$. All the eigenvalues λ_n can be shown to be independent of x [11,21,37].

The inverse scattering is achieved with the aid of the matrix function $K(x,t,s)$, defined by the equation:

$$\phi^-(x,t,\lambda) = \mathrm{e}^{\mathrm{i}\lambda Jt} + \int_{-\infty}^{t} K(x,t,s)\,\mathrm{e}^{\mathrm{i}\lambda Js}\,\mathrm{d}s, \tag{10}$$

whose validity follows from the asymptotic condition (8) for the Jost function $\phi^-(x,t,\lambda)$ at $t \to -\infty$. If we write the matrix function K in terms of its three columns $K = (\vec{K}_1, \vec{K}_2, \vec{K}_3)$, the Marchenko integral equations for these columns are computed to be [37,39]:

$$\sum_{j=2}^{3}\left[\vec{\mathbf{e}}_j F_j(x,t+y) + \int_{-\infty}^{t} \vec{K}_j(x,t,s)F_j(x,s+y)\,\mathrm{d}s\right] + \vec{K}_1(x,t,y) = 0, \tag{11a}$$

$$\vec{\mathbf{e}}_1 F_j^*(x,t+y) + \int_{-\infty}^{t} \vec{K}_1(x,t,s)F_j^*(x,s+y)\,\mathrm{d}s = \vec{K}_j(x,t,y), \quad j=2,3. \tag{11b}$$

Here, $\vec{\mathbf{e}}_j$ is the jth canonical unit vector in the three-dimensional Euclidean space, and $F_j(x,y)$ are the Marchenko kernels:

$$F_j(x,y) = \frac{1}{2\pi}\int_{-\infty}^{\infty} \mathrm{e}^{-\mathrm{i}\lambda y}\psi_j(x,\lambda)\,\mathrm{d}\lambda - \mathrm{i}\sum_{n=1}^{N}\beta_j(x,\lambda_n)\,\mathrm{e}^{-\mathrm{i}\lambda_n y}, \quad j=2,3, \tag{12}$$

where $\psi_j(x,\lambda) = S_{j1}(x,\lambda)/S_{11}(x,\lambda)$ are the reflection coefficients, and $\beta_j(x,\lambda_n)$ are the residues of $\psi_j(x,\lambda)$ at their poles $\lambda = \lambda_n$. The electric field envelopes $E_+(x,t)$ and $E_-(x,t)$ can be reconstructed from the elements of the matrix solution $K(x,t,s)$ as

$$E_+(x,t) = -4K_{21}^*(x,t,t), \qquad E_-(x,t) = -4K_{31}^*(x,t,t). \tag{13}$$

As mentioned above, the eigenvalues $\lambda_1,\ldots,\lambda_N$ do not depend on x. When all the eigenvalues λ_n are simple zeros of the matrix element $S_{11}(x,\lambda)$, the evolution equations for the residues $\beta_j(x,\lambda_n)$ have the form:

$$\frac{\mathrm{d}\beta_2}{\mathrm{d}x} = \frac{\mathrm{i}}{4}[(r_{22}-r_{11})\beta_2 + r_{23}\beta_3], \tag{14a}$$

$$\frac{\mathrm{d}\beta_3}{\mathrm{d}x} = \frac{\mathrm{i}}{4}[r_{32}\beta_2 + (r_{33}-r_{11})\beta_3]. \tag{14b}$$

Here, all the arguments of β_j and r_{jk} are (x,λ_n), and the coefficients r_{jk} are defined by

$$r_{11}(x,\lambda) = \mathcal{P}\int_{-\infty}^{\infty} \frac{\lim_{t\to-\infty}\mathcal{N}(x,t,\nu)g(\nu)}{\nu-\lambda}\,\mathrm{d}\nu, \tag{15a}$$

$$r_{22}(x,\lambda) = \mathcal{P}\int_{-\infty}^{\infty} \frac{\lim_{t\to-\infty}n_+(x,t,\nu)g(\nu)}{\nu-\lambda}\,\mathrm{d}\nu, \tag{15b}$$

$$r_{33}(x,\lambda) = \mathcal{P}\int_{-\infty}^{\infty} \frac{\lim_{t\to-\infty}n_-(x,t,\nu)g(\nu)}{\nu-\lambda}\,\mathrm{d}\nu, \tag{15c}$$

$$r_{23}(x,\lambda) = \mathcal{P}\int_{-\infty}^{\infty} \frac{\lim_{t\to-\infty}\mu(x,t,\nu)g(\nu)}{\nu-\lambda}\,\mathrm{d}\nu, \tag{15d}$$

$$r_{32}(x,\lambda) = \mathcal{P}\int_{-\infty}^{\infty} \frac{\lim_{t\to-\infty}\mu^*(x,t,\nu)g(\nu)}{\nu-\lambda}\,\mathrm{d}\nu. \tag{15e}$$

The evolution equations of the reflection coefficients $\psi_j(x,\lambda)$, $j=2,3$, with real λ, are given as

$$\frac{\partial\psi_2}{\partial x} = \frac{\mathrm{i}}{4}[(Q_{22}-Q_{11})\psi_2 + Q_{23}\psi_3 + 2\pi\mathrm{i}g(\lambda)R_+], \tag{16a}$$

$$\frac{\partial\psi_3}{\partial x} = \frac{\mathrm{i}}{4}[Q_{32}\psi_2 + (Q_{33}-Q_{11})\psi_3 + 2\pi\mathrm{i}g(\lambda)R_-], \tag{16b}$$

where

$$Q_{11}(x,\lambda) = r_{11}(x,\lambda) + \mathrm{i}\pi g(\lambda) \lim_{t\to-\infty} \mathcal{N}(x,t,\lambda), \tag{17a}$$

$$Q_{22}(x,\lambda) = r_{22}(x,\lambda) + \mathrm{i}\pi g(\lambda) \lim_{t\to-\infty} n_+(x,t,\lambda), \tag{17b}$$

$$Q_{33}(x,\lambda) = r_{33}(x,\lambda) + \mathrm{i}\pi g(\lambda) \lim_{t\to-\infty} n_-(x,t,\lambda), \tag{17c}$$

$$Q_{23}(x,\lambda) = r_{23}(x,\lambda) + \mathrm{i}\pi g(\lambda) \lim_{t\to-\infty} \mu(x,t,\lambda), \tag{17d}$$

$$Q_{32}(x,\lambda) = r_{32}(x,\lambda) + \mathrm{i}\pi g(\lambda) \lim_{t\to-\infty} \mu^*(x,t,\lambda) \tag{17e}$$

and

$$R_\pm(x,\lambda) = \lim_{t\to-\infty} \mathrm{e}^{2\mathrm{i}\lambda t} \rho_\pm^*(x,t,\lambda). \tag{18}$$

Recall that the last formula follows from the asymptotic condition (6). A derivation of the simplified version of Eqs. (16) with no initial medium polarizabilities,

$$\lim_{t\to-\infty} \rho_\pm(x,t,\lambda) = 0, \qquad \lim_{t\to-\infty} \mu(x,t,\lambda) = 0$$

was presented in [36].

The complete equations (16) are derived in a way very similar to the derivation of the analogous equations for the pure two-level Maxwell-Bloch system, presented in [21]. The details of this derivation will be included in a future publication.

If the broadening function $g(\lambda)$ is analytic near the real axis, we can use formulas (15) and (17) to rewrite $Q_{ij}(x,\lambda)$ as path integrals. For example,

$$Q_{11}(x,\lambda) = \int_{-\infty}^{\infty} \frac{\lim_{t\to-\infty}\mathcal{N}(x,t,\nu)g(\nu)}{\nu-\lambda-\mathrm{i}0}\,\mathrm{d}\nu,$$

where the symbol $-\mathrm{i}0$ in the denominator denotes an infinitesimal indentation of the integration path below the point $\nu = \lambda$. The remaining $Q_{ij}(x,\lambda)$ are evaluated via the same integral formula with the appropriate integrands in the numerator.

Eqs. (14), with $n = 1,\ldots,N$, and (16) give the x-evolution of all the relevant spectral data.

We conclude this section with a brief remark about solutions for which the electric field components $E_+(x,t)$ and $E_-(x,t)$ are real-valued. In particular, if these components are to be real, the resulting symmetry $U(x,t,\lambda) = U^*(x,t,-\lambda^*)$ of the scattering equation (5a) implies the equation $S(x,\lambda) = S^*(x,-\lambda^*)$ for the scattering matrix (9), and thus the equation $\psi_j(x,\lambda) = \psi_j^*(x,-\lambda^*)$ for the reflection coefficients $\psi_j(x,\lambda)$, $j = 2,3$. Therefore, if λ_n is a pole of the reflection coefficients $\psi_j(x,\lambda)$, then so is $-\lambda_n^*$, and for a simple pole $\lambda = \lambda_n$, the pole at $-\lambda_n^*$ must also be simple. Equating the appropriate Laurent expansions further implies the equations $\beta_j(x,\lambda_n) = -\beta_j^*(x,-\lambda_n^*)$ for the residues $\beta_j(x,\lambda_n)$ and $\beta_j^*(x,-\lambda_n^*)$, $j = 2,3$.

3.2. Polarization switching

In this section, we describe the polarization switching for optical pulses and pulse trains traveling through Λ-configuration media. We show this switching for the case of initial conditions (7) and when

$$\alpha_2(x,\lambda) = \lim_{t\to-\infty} [n_+(x,t,\lambda) - \mathcal{N}(x,t,\lambda)] \geq 0, \tag{19a}$$

$$\alpha_3(x,\lambda) = \lim_{t\to-\infty}\,[n_-(x,t,\lambda) - \mathcal{N}(x,t,\lambda)] \geq 0 \tag{19b}$$

and

$$\alpha_3(x,\lambda) - \alpha_2(x,\lambda) = \lim_{t\to-\infty}\,[n_-(x,t,\lambda) - n_+(x,t,\lambda)] \geq \Delta > 0 \tag{20}$$

for some number Δ and all x and λ, that is, if the $-$ sub-level is consistently more occupied than the $+$ sub-level as $t \to -\infty$, and both are more occupied than the excited level.

Under the initial conditions (7), both sets of evolution equations, (14) and (16), become decoupled, homogeneous, first-order linear equations, and can be easily solved. In particular, identically zero reflection coefficients:

$$\psi_j(x,\lambda) = \frac{S_{j1}(x,\lambda)}{S_{11}(x,\lambda)} \equiv 0, \quad j = 2,3 \tag{21}$$

are included among the solutions of (16) latter solutions are the N-soliton solutions. In this section, we first compute these, and show their polarization-switching property to hold when conditions (19) and (20) are satisfied. We then show that these same conditions lead to the zero reflection coefficient solution being asymptotically stable, which extends the switching property to arbitrary incoming pulses.

We first briefly describe the calculation of the N-soliton solutions from the Marchenko equations (11). The solutions of the evolution equations (14) for the residues $\beta_j(x,\lambda_n)$, with $j = 2,3$ and $n = 1,\ldots,N$, are given by

$$\beta_j(x,\lambda_n) = d_{nj}\,\mathrm{e}^{-\mathrm{i}D_j(x,\lambda_n)}, \quad j = 2,3, \tag{22}$$

where

$$D_j(x,\lambda) = \frac{1}{4}\int_0^x \mathrm{d}\xi\,\mathcal{P}\int_{-\infty}^{\infty}\frac{\alpha_j(\xi,\nu)g(\nu)}{\lambda-\nu}\,\mathrm{d}\nu, \quad j = 2,3 \tag{23}$$

and d_{nj}, $j = 2,3$, are constants. By using Eqs. (21) and (22), we find the Marchenko kernels (12) to be

$$F_j(x,y) = -\mathrm{i}\sum_{n=1}^{N} d_{nj}\,\mathrm{e}^{-\mathrm{i}\lambda_n y - \mathrm{i}D_j(x,\lambda_n)}, \quad j = 2,3.$$

We substitute these expressions into the Marchenko equations (11). After assuming

$$\vec{K}_1(x,t,y) = \sum_{n=1}^{N}\vec{K}_1^n(x,t)\,\mathrm{e}^{-\mathrm{i}\lambda_n y},$$

$$\vec{K}_j(x,t,y) = \sum_{n=1}^{N}\vec{K}_j^n(x,t)\,\mathrm{e}^{\mathrm{i}\lambda_n^* y}, \quad j = 2,3$$

and performing the appropriate integrations, we find that the Marchenko equations (11) become algebraic equations. For the two relevant components, K_{21} and K_{31}, of the vector $\vec{K}_1 = (K_{11}, K_{21}, K_{31})^{\mathrm{T}}$, we find

$$K_{j1}(x,t,t) = \frac{\det C_j}{\det B}, \quad j = 2,3, \tag{24}$$

where B is the $N \times N$ matrix with elements:

$$B_{nk} = \delta_{nk} - \sum_{j=1}^{N}\{d_{n2}d_{j2}^*\,\mathrm{e}^{-\mathrm{i}[D_2(x,\lambda_n)-D_2^*(x,\lambda_j)]} + d_{n3}d_{j3}^*\,\mathrm{e}^{-\mathrm{i}[D_3(x,\lambda_n)-D_3^*(x,\lambda_j)]}\}A_{kj}A_{nj},$$

$$A_{kj} = \frac{\mathrm{e}^{\mathrm{i}(\lambda_j^*-\lambda_k)t}}{\lambda_j^*-\lambda_k} \tag{25}$$

and the $(N+1)\times(N+1)$ matrices C_j, with $j=2,3$, are given by

$$C_j = \begin{pmatrix} 0 & \mathrm{e}^{-\mathrm{i}\lambda_1 t}\cdots\mathrm{e}^{-\mathrm{i}\lambda_N t} \\ -\mathrm{i}d_{1j}\,\mathrm{e}^{-\mathrm{i}\lambda_1 t-\mathrm{i}D_j(x,\lambda_1)} & \\ \vdots & B \\ -\mathrm{i}d_{Nj}\,\mathrm{e}^{-\mathrm{i}\lambda_N t-\mathrm{i}D_j(x,\lambda_N)} & \end{pmatrix}. \tag{26}$$

Eqs. (13) then yield the electric field envelopes $E_+(x,t)$ and $E_-(x,t)$ as

$$E_+(x,t) = -4K^*_{21}(x,t,t), \qquad E_-(x,t) = -4K^*_{31}(x,t,t). \tag{27}$$

To establish the switching property, let us first notice that (20) and (23) imply

$$\mathrm{Im}[D_2(x,\lambda_n) - D_3(x,\lambda_n)] = \frac{\mathrm{Im}\,\lambda_n}{4}\int_0^x \mathrm{d}\xi \int_{-\infty}^{\infty} \frac{[\alpha_3(\xi,\nu)-\alpha_2(\xi,\nu)]g(\nu)}{|\nu-\lambda_n|^2}\,\mathrm{d}\nu \to \infty \tag{28}$$

as $x\to\infty$, due to $\mathrm{Im}\,\lambda_n > 0$. Moreover, we notice that the determinants of the matrices C_j, given by (26), can be expanded in terms of their first columns as

$$\det C_j = \mathrm{i}\sum_{n=1}^{N}(-1)^{n+1}d_{nj}\,\mathrm{e}^{-\mathrm{i}D_j(x,\lambda_n)}C^{(n+1)},$$

where $C^{(n+1)}$ is the minor corresponding to the $(n+1)$st element in the first column of the matrix C_j multiplied by $\mathrm{e}^{-\mathrm{i}\lambda_n t}$, and is the same for both $j=2$ and $j=3$. If the N-soliton solution is non-degenerate, all $d_{n2}\neq 0$. Because of this and (28), as $x\to\infty$, the terms in the determinant $\det C_2$ are exponentially large compared with the equivalent terms in the determinant $\det C_3$. Therefore, from Eqs. (27), (25), (26) and (24), one sees that, in the corresponding N-soliton solution, the component $E_-(x,t)$ is in general negligible compared to the component $E_+(x,t)$ for large values of x.

In addition, condition (20) and definition (23) imply

$$\begin{aligned}&\mathrm{Im}[D_2(x,\lambda_n) - D_2^*(x,\lambda_m)] - \mathrm{Im}[D_3(x,\lambda_n) - D_3^*(x,\lambda_m)] \\ &\quad = \frac{1}{4}\int_0^x \mathrm{d}\xi \int_{-\infty}^{\infty}[\alpha_3(\xi,\nu)-\alpha_2(\xi,\nu)]\left[\frac{\mathrm{Im}\,\lambda_n}{|\nu-\lambda_n|^2} + \frac{\mathrm{Im}\,\lambda_m}{|\nu-\lambda_m|^2}\right] g(\nu)\,\mathrm{d}\nu \to \infty.\end{aligned}$$

Therefore, as $x\to\infty$, all the terms with $j=3$ in formula (25) are exponentially small compared to the corresponding terms with $j=2$. Together with the result of the preceding paragraph, this implies that the limiting electric field $E_+(x,t)$ becomes the N-soliton solution of the two-level Maxwell–Bloch sub-system that corresponds exclusively to the transition between the + ground sub-level and the excited level, while the limiting electric field $E_-(x,t)$ vanishes.

We now show that, if

$$\alpha_j(x,\lambda) > 0, \quad j=1,2, \tag{29}$$

that is, if each of the ground states is more populated than the excited state, the N-soliton solutions are asymptotically stable, except in the sharp-line case $g(\lambda)=\delta(\lambda)$, when they are only stable. (Our treatment largely follows that of [11] for two-level systems.) Thus, in this case, when condition (20) is satisfied, any input pulse indeed asymptotically becomes an N-soliton solution of the two-level sub-system corresponding to the transition between the + ground sub-level and the excited level.

We recall that an N-soliton solution, given by formulas (27), (25), (26) and (24), is stable if any continuous radiation part with the same initial data (15) stays small with increasing distance x, and is asymptotically stable if the continuous radiation vanishes with increasing x. To show that the N-soliton solutions indeed satisfy this stability criterion, since we have assumed the initial conditions (7), we use the homogeneous versions of Eqs. (16) with vanishing off-diagonal coefficients Q_{23} and Q_{32}. As noted at the beginning of this section, these equations decouple, and can be solved easily. If we recall the definitions (19) and (23) for $\alpha_j(x,\lambda)$ and $D_j(x,\lambda)$, $j=2,3$, respectively, we find from the corresponding equations (16) the reflection coefficients $\psi_2(x,\lambda)$ and $\psi_3(x,\lambda)$ to be

$$\psi_j(x,\lambda) = \psi_j(0,\lambda)\exp\left\{-\frac{\pi}{4}g(\lambda)\int_0^x \alpha_j(\xi,\lambda)\,\mathrm{d}\xi - \mathrm{i}D_j(x,\lambda)\right\}, \quad j=2,3. \tag{30}$$

Since, by assumption (29), $\alpha_j(x,\lambda) > 0$ for all x and real λ, and since, for real λ, both $D_2(x,\lambda)$ and $D_3(x,\lambda)$ are real, the reflection coefficients decay with x for all finite broadening distribution functions $g(\lambda)$. An application of the Lebesgue Dominated Convergence Theorem shows that (if $|\psi_2(0,\lambda)|$ and $|\psi_3(0,\lambda)|$ have finite integrals along the λ-axis) the contribution of the continuous radiation to the Marchenko kernels (12) also decays with x. Thus, N-soliton solutions are indeed not only stable but in fact asymptotically stable for large distances x.

It is interesting to notice that Eq. (30) implies the contribution of the more excited ground sub-level to the continuous radiation part of the Marchenko kernel (12) to become exponentially small compared to that of the less excited ground sub-level. We remark that similar analysis should therefore also show an analogous switching property in the amplifier case, in which the continuous radiation dominates.

In the limiting sharp-line case $g(\lambda) = \delta(\lambda)$, away from $\lambda = 0$, where there is a singularity, the reflection coefficients $\psi_2(x,\lambda)$ and $\psi_3(x,\lambda)$ become

$$\psi_j(x,\lambda) = \psi_j(0,\lambda)\exp\left\{-\frac{\mathrm{i}}{4\lambda}\int_0^x \alpha_j(\xi,\lambda)\,\mathrm{d}\xi\right\}, \quad j=2,3$$

which implies that in this limit the reflection coefficients oscillate, but do not grow. The N-soliton solutions are therefore only stable. Thus, in the sharp-line limit, we can only claim the polarization-switching property and the asymptotic non-degenerate two-level behavior for N-soliton solutions.

If $\alpha_2(x,\lambda) = 0$ and $\alpha_3(x,\lambda) > 0$, an interesting limiting case occurs. In particular, both soliton and continuous radiation components of the field $E_-(x,t)$ vanish as $x \to \infty$ by the arguments presented in the preceding paragraphs. On the other hand, the limiting behavior of the field $E_+(x,t)$ becomes independent of x. Its asymptotic shape becomes that given by the initial reflection coefficient $\psi_2(x,\lambda)$ and initial residues d_{2n} in the corresponding two-level problem. Formulas (2) show that, in the laboratory frame, this field is being translated at the speed of light without changing shape.

Clearly, the above results remain true if the indices 2 and 3, and $+$ and $-$, are interchanged. The preceding discussion implies, in other words, that in such a situation, deep inside the medium, the light is indeed purely circularly polarized, and that the direction of its polarization depends solely on the occupation numbers of the two degenerate ground sub-levels.

3.3. One-soliton solution

In this section, we illustrate the general results of the preceding section on the simplest, one-soliton solutions. Each such solution corresponds to a single zero, $\lambda_1 = \gamma + \mathrm{i}\mu$, of the element $S_{11}(\lambda)$ in the upper half-plane, $\mathrm{Im}\,\lambda > 0$. For simplicity, we assume that the inhomogeneous broadening $g(\lambda)$ is given by the Lorentzian:

$$g(\lambda) = \frac{\varepsilon}{\pi(\varepsilon^2+\lambda^2)}, \tag{31}$$

where ε is a positive parameter. Note that as $\varepsilon \to 0$, we recover the unbroadened, or sharp-line, limit $g(\lambda) = \delta(\lambda)$.

We first restrict ourselves to the simplest special case in which only the degenerate sub-levels are populated as $t \to -\infty$, and the population densities are space-independent. In this case:

$$\lim_{t\to-\infty} \mathcal{N}(x,t,\lambda) = 0, \qquad \lim_{t\to-\infty} n_+(x,t,\lambda) = \alpha_2, \qquad \lim_{t\to-\infty} n_-(x,t,\lambda) = \alpha_3. \tag{32}$$

We remark that the assumption (32) yields the same solutions as the more general assumption:

$$\lim_{t\to-\infty} (n_+ - \mathcal{N})(x,t,\lambda) = \alpha_2, \qquad \lim_{t\to-\infty} (n_- - \mathcal{N})(x,t,\lambda) = \alpha_3,$$

where $\lim_{t\to-\infty} \mathcal{N}(x,t,\lambda)$ is an arbitrary function of x and λ, so long as α_2 and α_3 are constant.

We solve the principal value integrals (23) and find

$$D_j(x,\lambda_n) = \frac{\alpha_j x}{4(\lambda_n + \mathrm{i}\varepsilon)}, \quad j = 2,3, \tag{33}$$

where, in our case, we only consider $n = 1$. We substitute (33) and the value $\lambda_1 = \gamma + \mathrm{i}\mu$ into Eqs. (25), (26), (24) and (27), to obtain the one-soliton solution:

$$E_+(x,t) = -\frac{4\mathrm{i}\mu d_2^* \,\mathrm{e}^{\mathrm{i}\Omega_2}}{\sqrt{|d_2|^2 + |d_3|^2\,\mathrm{e}^{2\Delta\theta}}} \operatorname{sech}\theta, \tag{34a}$$

$$E_-(x,t) = -\frac{4\mathrm{i}\mu d_3^* \,\mathrm{e}^{\mathrm{i}\Omega_3}}{\sqrt{|d_2|^2\,\mathrm{e}^{-2\Delta\theta} + |d_3|^2}} \operatorname{sech}\theta \tag{34b}$$

with

$$\theta = \theta_2 - \theta_{02}(x) = \theta_3 - \theta_{03}(x), \tag{35a}$$

$$\Omega_j = 2\gamma t + \frac{\gamma\alpha_j x}{4[\gamma^2 + (\mu+\varepsilon)^2]}, \qquad \theta_j = 2\mu t + \frac{(\mu+\varepsilon)\alpha_j x}{4[\gamma^2 + (\mu+\varepsilon)^2]}, \quad j = 2,3, \tag{35b}$$

$$\theta_{02}(x) = \ln\frac{2\mu}{\sqrt{|d_2|^2 + |d_3|^2\,\mathrm{e}^{2\Delta\theta}}}, \qquad \theta_{03}(x) = \ln\frac{2\mu}{\sqrt{|d_2|^2\,\mathrm{e}^{-2\Delta\theta} + |d_3|^2}} \tag{35c}$$

and

$$\Delta\theta = \theta_3 - \theta_2 = \frac{(\mu+\varepsilon)(\alpha_2 - \alpha_3)x}{4[\gamma^2 + (\mu+\varepsilon)^2]}. \tag{35d}$$

This solution and its dynamics were first described in [25]. The analogous solution for V-configuration media was obtained in [30] and applied to studying frequency conversion.

Asymptotically, for the initial population densities $\alpha_2 > \alpha_3$ and for

$$x \gg x_0 = 4\frac{[\gamma^2 + (\mu+\varepsilon)^2]}{(\mu+\varepsilon)(\alpha_2 - \alpha_3)}, \tag{36}$$

we find that the soliton solution (34) behaves as

$$E_+(x,t) \to 0, \qquad E_-(x,t) \to -\frac{4\mathrm{i}\mu d_3^* \,\mathrm{e}^{\mathrm{i}\Omega_3}}{|d_3|} \operatorname{sech}\left(\theta_3 - \ln\frac{2\mu}{|d_3|}\right). \tag{37}$$

For $\alpha_2 < \alpha_3$, we obtain the same result, with 2 and 3, and + and −, interchanged. Indeed, this is the predicted polarization switching. For a special choice of parameters, solution (34), which illustrates this switching process, is shown in Fig. 2.

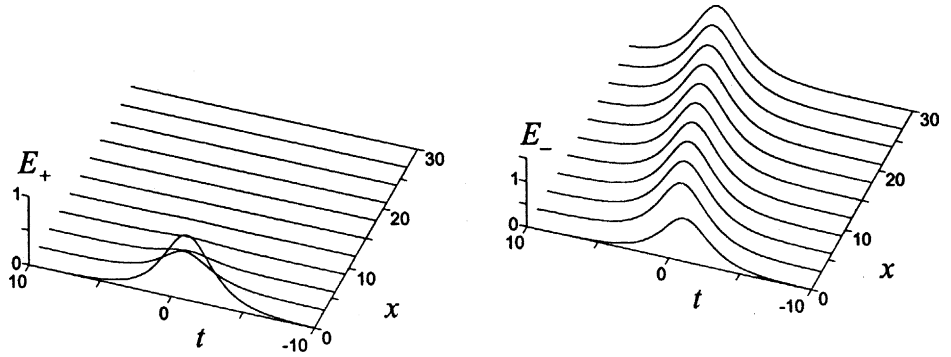

Fig. 2. The simplest one-soliton solution of the type given by Eq. (34) with parameters $\gamma = 0$, $\mu = 1/3$, $\varepsilon = 0$, $\alpha_2 = 5/6$, $\alpha_3 = 1/6$, $d_2 = d_3 = -\mathrm{i}$.

If $\alpha_2 = \alpha_3$, we find $\theta_2 = \theta_3 \equiv \bar{\theta}$, $\Omega_2 = \Omega_3 \equiv \bar{\Omega}$, and $\Delta\theta = 0$. In this case,

$$E_{\pm}(x,t) = -\frac{4\mathrm{i}\mu d_j^* \, \mathrm{e}^{\mathrm{i}\bar{\Omega}}}{\sqrt{|d_2|^2 + |d_3|^2}} \operatorname{sech}\left(\bar{\theta} - \ln \frac{2\mu}{\sqrt{|d_2|^2 + |d_3|^2}}\right)$$

for all x and t, where $j = 2$ in $E_+(x,t)$ and $j = 3$ in $E_-(x,t)$. In other words, when the two initial populations α_2 and α_3 are equal, both polarizations of the electric field survive, and travel together as phase-modulated sech-like waves, so there is no switching in this case.

Recall that our formulas for the soliton describe it in the light-cone (x,t)-coordinate frame that travels to the right with the speed of light $c = 1$. To transform the soliton to the more natural laboratory (X,T)-coordinate frame, we use the transformation (2), $x = X$, $t = T - X$. In these coordinates, we see that the soliton travels with the velocity:

$$v = \left\{1 + \frac{(\mu+\varepsilon)\alpha}{8\mu[\gamma^2 + (\mu+\varepsilon)^2]}\right\}^{-1},$$

where $\alpha = \alpha_3$ if $\alpha_2 > \alpha_3$, $\alpha = \alpha_2$ if $\alpha_2 < \alpha_3$, and $\alpha = \alpha_2 = \alpha_3$ if $\alpha_2 = \alpha_3$. As expected, this velocity is less than the speed of light.

Note that the asymptotic soliton velocity, v, increases with ε. In particular, in the infinite-broadening limit, $\varepsilon \to \infty$, the velocity v approaches the speed of light. Moreover, the shape of both soliton components remains unchanged during the propagation along the x-axis. From Eq. (33), we see that the same is true for an N-soliton solution: in the light-cone (x,t)-coordinate frame, as $\varepsilon \to \infty$, the N-soliton solution loses its x-dependence, which, in the laboratory (X,T)-coordinates corresponds to rigid translation of the initial shape with the speed of light. Thus, in the infinite-broadening limit, all the N-soliton solutions behave in the same way as solutions of the linear wave equation.

To determine the actual length of the medium needed for the complete switching of the soliton's polarization to circular, let us again first assume that $\alpha_2 > \alpha_3$, and recall formula (36). In reality, $x \approx 5x_0$, with x_0 given in (36), will suffice for the E_+-component of the soliton pulse to almost completely vanish, and for the E_--component to become indistinguishable from the form (37). We notice that the quantities:

$$x_j = 4\frac{[\gamma^2 + (\mu+\varepsilon)^2]}{(\mu+\varepsilon)\alpha_j}, \quad j = 2,3$$

are the spatial widths of the two polarization components, $E_{\pm}(x,t)$, of the soliton pulse shortly after it enters the medium. Formula (36) shows that the length x_0 can be computed as

$$\frac{1}{x_0} = \frac{1}{x_2} - \frac{1}{x_3}$$

and, in general,

$$\frac{1}{x_0} = \left| \frac{1}{x_2} - \frac{1}{x_3} \right|.$$

In other words, the inverse "switching length" is proportional to the absolute value of the difference between the inverse spatial widths of the two pulse components.

We now consider a more interesting one-soliton case in which almost complete switching of polarization from one circular component to another is achieved by tuning the initial populations of the two degenerate sub-levels. For this case, we assume

$$\lim_{t\to-\infty} \mathcal{N}(x,t,\lambda) = 0, \tag{38a}$$

$$\lim_{t\to-\infty} n_+(x,t,\lambda) = \begin{cases} \alpha_2, & x < L, \\ \beta_2, & x > L, \end{cases} \tag{38b}$$

$$\lim_{t\to-\infty} n_-(x,t,\lambda) = \begin{cases} \alpha_3, & x < L, \\ \beta_3, & x > L, \end{cases} \tag{38c}$$

where α_j, β_j, $j = 2, 3$, and L are constants, with $\alpha_2 > \alpha_3$ and $\beta_2 < \beta_3$. These initial conditions represent a physical setup in which the occupation numbers of the two ground sub-levels change at a distance L into the medium, so that the roles of the more- and less-populated sub-levels switch at that point.

Formulae (34) are still valid in this case, but now with

$$\Omega_j = \begin{cases} 2\gamma t + \dfrac{\gamma\alpha_j x}{4[\gamma^2 + (\mu+\varepsilon)^2]}, & x < L, \\ 2\gamma t + \dfrac{\gamma[\alpha_j L + \beta_j (x-L)]}{4[\gamma^2 + (\mu+\varepsilon)^2]}, & x > L, \end{cases} \qquad j = 2, 3, \tag{39a}$$

$$\theta_j = \begin{cases} 2\mu t - \dfrac{(\mu+\varepsilon)\alpha_j x}{4[\gamma^2 + (\mu+\varepsilon)^2]}, & x < L, \\ 2\mu t - \dfrac{(\mu+\varepsilon)[\alpha_j L + \beta_j (x-L)]}{4[\gamma^2 + (\mu+\varepsilon)^2]}, & x > L, \end{cases} \qquad j = 1, 2, \tag{39b}$$

$$\Delta\theta = \begin{cases} \dfrac{(\mu+\varepsilon)(\alpha_2 - \alpha_3)x}{4[\gamma^2 + (\mu+\varepsilon)^2]}, & x < L, \\ \dfrac{(\mu+\varepsilon)[(\alpha_2 - \alpha_3)L + (\beta_2 - \beta_3)(x-L)]}{4[\gamma^2 + (\mu+\varepsilon)^2]}, & x > L. \end{cases} \tag{39c}$$

If

$$L \gg 4\frac{[\gamma^2 + (\mu+\varepsilon)^2]}{(\mu+\varepsilon)(\alpha_2 - \alpha_3)},$$

then for $0 \ll x < L$, the soliton becomes exponentially close to the form (37). In particular, only the component $E_-(x,t)$ is present. After the switch at $x = L$, for

$$x \gg \left(1 + \frac{\alpha_2 - \alpha_3}{\beta_3 - \beta_2}\right) L,$$

the soliton behaves as

$$E_+(x,t) \to -\frac{4\mathrm{i}\mu d_2^* \, \mathrm{e}^{\mathrm{i}\Omega_2}}{|d_2|} \operatorname{sech}\left(\theta_2 - \ln\frac{2\mu}{|d_2|}\right), \qquad E_-(x,t) \to 0.$$

This asymptotic solution has an additional shift:

$$\Delta x = \frac{(\mu+\varepsilon)(\alpha_2 - \beta_2)L}{8\mu[\gamma^2 + (\mu+\varepsilon)^2]},$$

in the position of the soliton center as compared to the solution in which the respective initial occupation numbers are β_2 and β_3 throughout the medium. It is also important to notice that the amplitude of the soliton, 4μ, does not change through the switch.

A one-soliton solution of the type just described is shown in Fig. 3, which contains a dramatic demonstration of the switching property. Notice how the E_+-component vanishes almost completely for $x < L$ but eventually recovers for large x and saturates to contain all the light, while the E_--component for $x < L$ grows and saturates to contain almost all the light, changes speed at $x = L$ and stays at approximately the same amplitude until approximately $x = 2L$, and then decays and eventually vanishes for large x.

3.4. Examples of switching in multi-soliton solutions

It follows from the results of Section 3.2 that multi-soliton solutions should exhibit the polarization-switching property in a manner similar to the one-soliton solutions. In this section, we illustrate this fact on two examples. We use the same notation $\lambda_j = \gamma_j + \mathrm{i}\mu_j$, $j = 1, \ldots, N$, for the eigenvalues as in the previous section. We again assume the Lorentzian form (31) for the broadening function $g(\lambda)$.

In order to simplify the presentation, we first discuss conditions under which the two electric field components $E_+(x,t)$ and $E_-(x,t)$ of an N-soliton solution are real. From the remark made at the end of Section 3.1, it follows that all of the eigenvalues λ_n and the corresponding coefficients d_{nj}, $j = 2, 3$, in formulas (27), obtained from (25), (26) and (24), which describe such an N-soliton solution, must fall into precisely two categories: either $\lambda_n = \mathrm{i}\mu_n$ is

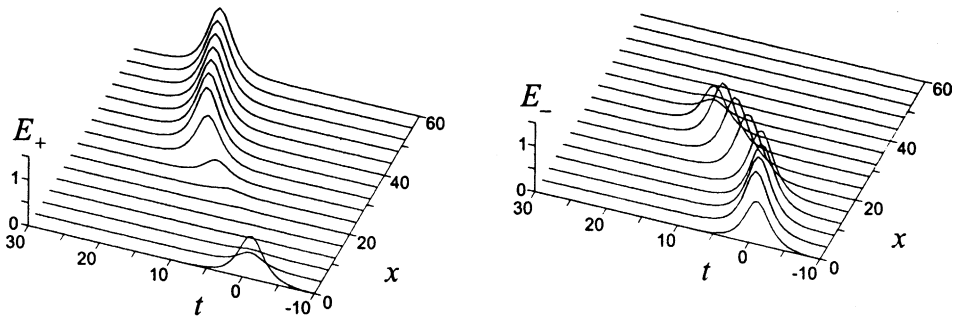

Fig. 3. A one-soliton solution of the type given by Eqs. (34) and (39) with parameters $\gamma = 0$, $\mu = 1/3$, $\varepsilon = 1/10$, $L = 15$, $\alpha_2 = 5/6$, $\alpha_3 = 1/6$, $\beta_2 = 1/5$, $\beta_3 = 4/5$, $d_2 = d_3 = -\mathrm{i}$.

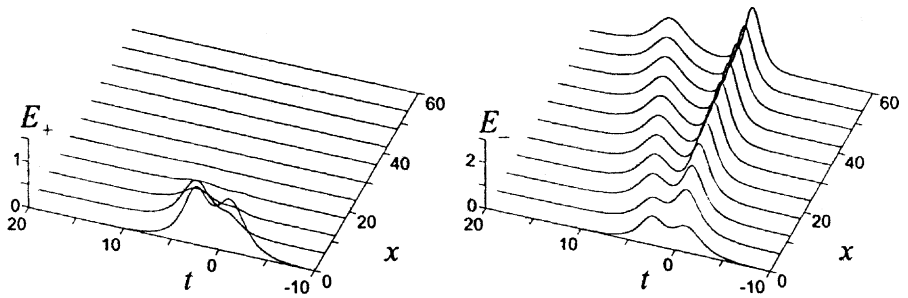

Fig. 4. A two-soliton solution with parameters $\gamma_1 = \gamma_2 = 0$, $\mu_1 = 1/3$, $\mu_2 = 2/3$, $\varepsilon = 1/10$, $\alpha_2 = 5/6$, $\alpha_3 = 1/6$, $d_{j2} = d_{j3} = -\mathrm{i}$, $j = 1, 2$.

purely imaginary and so are d_{nj}, $j = 2, 3$, or else $\lambda_n = \gamma_n + \mathrm{i}\mu_n$, $\lambda_{n+1} = -\gamma_n + \mathrm{i}\mu_n = -\lambda_n^*$ and $d_{(n+1)j} = -d_{nj}^*$. If such an N-soliton solution corresponds to K purely imaginary eigenvalues and M eigenvalue pairs satisfying the relations $\lambda_{2n} = -\lambda_{2n-1}^*$, $n = 1, \ldots, M$, it is customary to say that it contains K-solitons, or 2π-pulses, and M breathers, or 0π-pulses. Due to the switching property that we showed in Section 3.2, the asymptotics of a solution composed of these solitons and breathers are, in general, the same as for the corresponding solutions of the non-degenerate two-level Maxwell–Bloch equations, which are described in [12,14]. In particular, for large x, the entire solution can be decomposed into K well-separated sech-like soliton components and M isolated breathers. The latter, whose specific from is shown for instance in formula (39) in [11], are periodic in x and resemble a pair of single solitons with different widths and amplitudes of different signs passing through one-another in a periodic fashion.

The first example is a two-soliton solution with real values of the electric field components $E_+(x, t)$ and $E_-(x, t)$. Fig. 4 shows this solution in the case of constant initial occupations of the degenerate ground sub-levels, while Fig. 5 shows it in the case when the initial occupations of the degenerate ground sub-levels are step functions described by formulas (38). In Fig. 4, the two humps of $E_+(x, t)$ decay and those of $E_-(x, t)$ grow and then saturate into two sech-like solutions traveling with different speeds. In Fig. 5, the humps of $E_+(x, t)$ decay and those of $E_-(x, t)$ grow for $x < L$. After that, $E_+(x, t)$ grows and saturates while $E_-(x, t)$ decays and vanishes.

The second example is a solution with real values of the electric field components $E_+(x, t)$ and $E_-(x, t)$ that contains a soliton and a breather. Fig. 6 shows this solution for constant initial occupations of the degenerate ground sub-levels, and Fig. 7 shows it for step-like initial occupations of the degenerate ground sub-levels as described by formulas (38). Again, in Fig. 6, the component $E_+(x, t)$ decays and $E_-(x, t)$ grows and saturates for large x, while in Fig. 7 the solution behaves similarly to that in Fig. 6 for $x < L$ and reverses the growth and decay of the two electric field components for $x > L$.

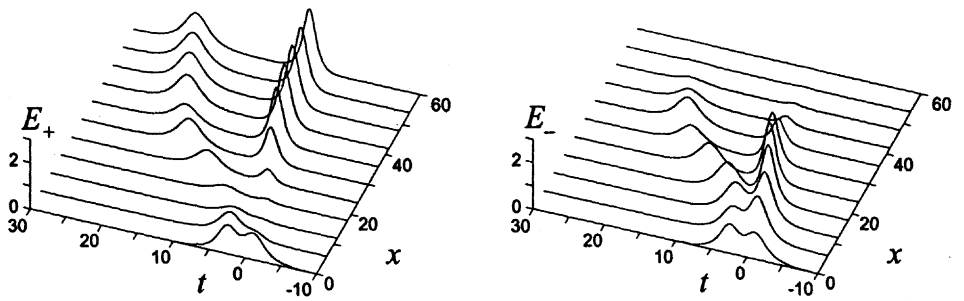

Fig. 5. A two-soliton solution with step-like initial populations, as described by formulas (38), and parameters $\gamma_1 = \gamma_2 = 0$, $\mu_1 = 1/3$, $\mu_2 = 2/3$, $\varepsilon = 1/10$, $L = 15$, $\alpha_2 = 5/6$, $\alpha_3 = 1/6$, $\beta_2 = 1/5$, $\beta_3 = 4/5$, $d_{j2} = d_{j3} = -\mathrm{i}$, $j = 1, 2$.

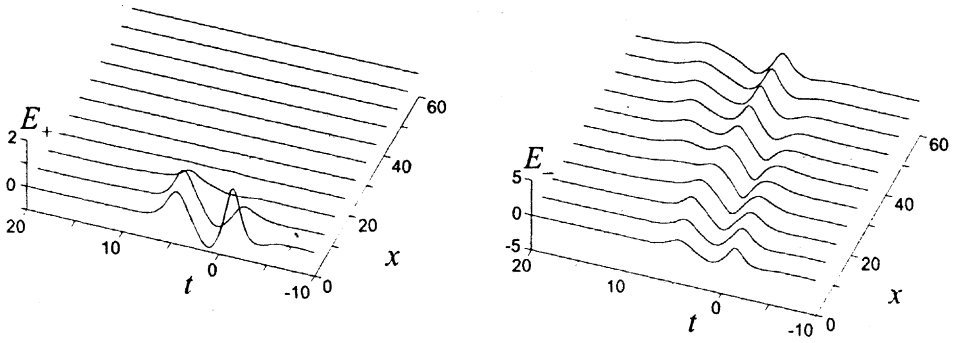

Fig. 6. A soliton-breather solution with parameters $\gamma_1 = 0$, $\gamma_2 = 1/3$, $\gamma_3 = -1/3$, $\mu_j = 1/3$, $\varepsilon = 1/10$, $\alpha_2 = 5/6$, $\alpha_3 = 1/6$, $d_{j2} = d_{j3} = -\mathrm{i}$, $j = 1, 2, 3$.

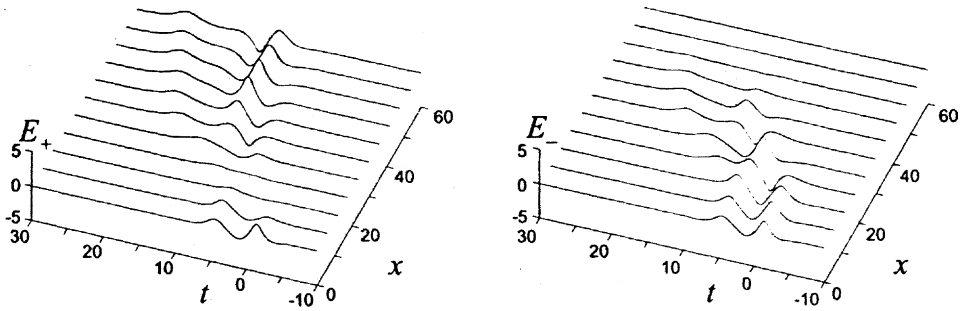

Fig. 7. A soliton-breather solution with step-like initial populations, as described by formulas (38), and parameters $\gamma_1 = 0$, $\gamma_2 = 1/3$, $\gamma_3 = -1/3$, $\mu_j = 1/3$, $\varepsilon = 1/10$, $L = 15$, $\alpha_2 = 5/6$, $\alpha_3 = 1/6$, $\beta_2 = 1/5$, $\beta_3 = 4/5$, $d_{j2} = d_{j3} = -\mathrm{i}$, $j = 1, 2, 3$.

4. Polarization dynamics

In this section, we study the polarization dynamics exhibited by the light interacting with a Λ-configuration resonant active optical medium by using the standard concepts from the theory of polarized plane waves, the polarization ellipse and the Stokes' variables on the Poincaré sphere. These concepts help to describe the details of the polarization dynamics of the light pulses under investigation at any point along the medium and at any moment in time. In particular, we show that polarization dynamics of the one-soliton solutions are independent of time, and thus have particularly simple representations on the Poincaré sphere.

4.1. Polarized plane waves

For completeness, we here review the basic concepts from the theory of polarized light. Standard references on this topic are [40,41]. We consider a plane electromagnetic wave with frequency ω and wave number k, propagating in the positive x direction. This wave has the form:

$$\vec{\mathcal{E}}(x,t) = \begin{pmatrix} \mathcal{E}_y(x,t) \\ \mathcal{E}_z(x,t) \end{pmatrix} = \mathrm{Re}\{\vec{E}\,\mathrm{e}^{\mathrm{i}(kx-\omega t)}\} = \begin{pmatrix} |E_y|\cos(kx-\omega t+\varphi_y) \\ |E_z|\cos(kx-\omega t+\varphi_z) \end{pmatrix}. \tag{40}$$

Here, $\vec{E} = (E_y, E_z)^{\mathrm{T}} = (|E_y|\,\mathrm{e}^{\mathrm{i}\varphi_y}, |E_z|\,\mathrm{e}^{\mathrm{i}\varphi_z})^{\mathrm{T}}$ is the vector of the complex wave amplitudes.

As the plane wave propagates in the positive x direction, an observer standing along the x-axis looking at the $y-z$ plane, which contains the electric field vector $\vec{\mathcal{E}}(x,t)$, will see the electric field vector trace out an ellipse. This can be shown as follows. First, we define the circular polarization basis vectors $\vec{\mathbf{e}}_+$ and $\vec{\mathbf{e}}_-$ in terms of the cartesian basis vectors $\vec{\mathbf{e}}_y$ and $\vec{\mathbf{e}}_z$ in the $y-z$ plane as

$$\vec{\mathbf{e}}_+ = \frac{1}{\sqrt{2}}\left(\vec{\mathbf{e}}_y + \mathrm{i}\vec{\mathbf{e}}_z\right), \qquad \vec{\mathbf{e}}_- = \frac{1}{\sqrt{2}}(\vec{\mathbf{e}}_y - \mathrm{i}\vec{\mathbf{e}}_z).$$

Note that these vectors satisfy the complex orthogonality relations $\vec{\mathbf{e}}_\pm \cdot \vec{\mathbf{e}}_\pm^* = 1$, $\vec{\mathbf{e}}_\pm \cdot \vec{\mathbf{e}}_\mp^* = 0$, with the dot denoting the usual real dot product. For a complex electric field amplitude given in components as

$$\vec{E} = E_y\,\vec{\mathbf{e}}_y + E_z\,\vec{\mathbf{e}}_z = E_+\,\vec{\mathbf{e}}_+ + E_-\,\vec{\mathbf{e}}_-, \tag{41}$$

the transformation formulae between the two sets of components are

$$E_y = \frac{1}{\sqrt{2}}(E_+ + E_-), \qquad E_z = \frac{\mathrm{i}}{\sqrt{2}}(E_+ - E_-). \tag{42}$$

The general form of the complex electric field amplitude $\vec{E}$ is given by the formula:

$$\vec{E} = |E_+|\,\mathrm{e}^{\mathrm{i}\phi}\,\vec{\mathbf{e}}_+ + |E_-|\,\mathrm{e}^{\mathrm{i}(\phi+2\psi)}\,\vec{\mathbf{e}}_- = (|E_+|\,\mathrm{e}^{-\mathrm{i}\psi}\,\vec{\mathbf{e}}_+ + |E_-|\,\mathrm{e}^{\mathrm{i}\psi}\,\vec{\mathbf{e}}_-)\,\mathrm{e}^{\mathrm{i}(\phi+\psi)} \tag{43}$$

which yields the electric field

$$\begin{aligned}\vec{\mathcal{E}} = {} & \frac{|E_+| + |E_-|}{\sqrt{2}}(\cos\psi\,\vec{\mathbf{e}}_y + \sin\psi\,\vec{\mathbf{e}}_z)\,\cos(kx - \omega t + \phi + \psi) \\ & - \frac{|E_+| - |E_-|}{\sqrt{2}}(-\sin\psi\,\vec{\mathbf{e}}_y + \cos\psi\,\vec{\mathbf{e}}_z)\sin(kx - \omega t + \phi + \psi).\end{aligned}$$

This field clearly traces out an ellipse whose major semi-axis encloses the angle ψ with the y-axis. The angle ψ is called the polarization azimuth, and takes on values $0 \le \psi \le \pi$. The ratio of the semi-axes of the ellipse is

$$\left|\frac{|E_+| - |E_-|}{|E_+| + |E_-|}\right|.$$

Given this ratio, the angle of ellipticity, η, is computed from the formula:

$$\tan\eta = \frac{|E_+| - |E_-|}{|E_+| + |E_-|}. \tag{44}$$

This angle takes on values $-\pi/4 \le \eta \le \pi/4$. Its magnitude is found by enclosing the polarization ellipse in a box and measuring the angle between the major axis of the ellipse and the main diagonal of the box (see Fig. 8). Its sign represents the sense of rotation of the electric field $\vec{\mathcal{E}}(x,t)$ along the perimeter of the ellipse.

Special cases of Eq. (43) include linear polarization when $\eta = 0$, that is $|E_+| = |E_-|$, and circular polarization. In particular, the field $\vec{\mathcal{E}}(x,t)$ is left-circularly polarized if $\eta = -\pi/4$, that is $|E_+| = 0$, and right-circularly polarized if $\eta = \pi/4$, that is $|E_-| = 0$.

An alternative representation of polarized light is furnished by the Stokes parameters:

$$S_0 = |E_y|^2 + |E_z|^2 = |E_+|^2 + |E_-|^2, \tag{45a}$$

$$S_1 = |E_y|^2 - |E_z|^2 = E_+E_-^* + E_-E_+^*, \tag{45b}$$

$$S_2 = E_yE_z^* + E_zE_y^* = \mathrm{i}(E_+E_-^* - E_-E_+^*), \tag{45c}$$

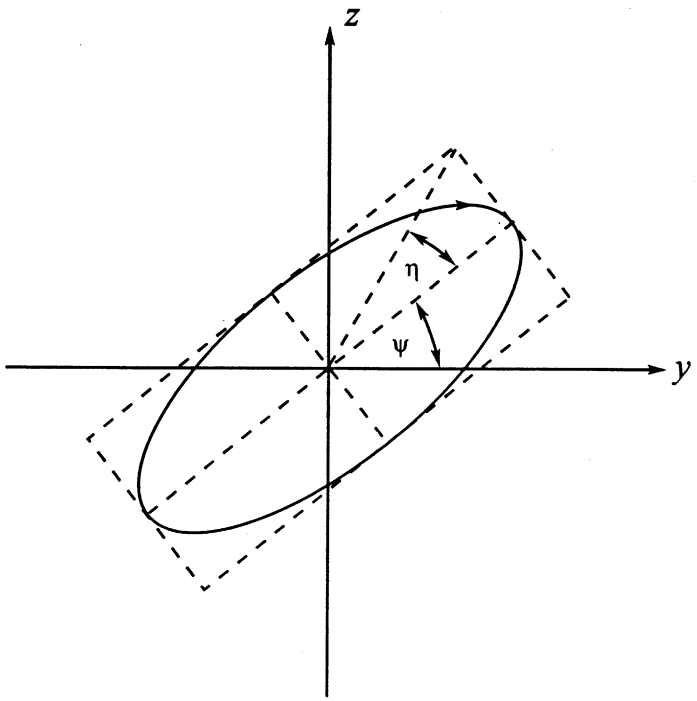

Fig. 8. Polarization ellipse in the plane perpendicular to the propagation of light.

$$S_3 = \mathrm{i}(E_y E_z^* - E_z E_y^*) = |E_+|^2 - |E_-|^2. \tag{45d}$$

(see, for example [41]). These parameters are not independent, since the intensity of light, S_0, can be expressed in terms of the rest of the parameters via the Pythagorean theorem $S_0^2 = S_1^2 + S_2^2 + S_3^2$. For studying the polarization of the light wave, we normalize the last three Stokes parameters to obtain the Stokes vector that lies on the unit sphere:

$$\vec{s} = (s_1, s_2, s_3)^{\mathrm{T}} = \frac{(S_1, S_2, S_3)^{\mathrm{T}}}{S_0}. \tag{46}$$

This sphere is also known as the Poincaré sphere for the complex field amplitudes E_+ and E_-.

To relate the location of the point $\vec{s}$ in cartesian coordinates to the angles ψ and η, which identify the polarization state, we first notice that $S_1 = 2|E_+||E_-|\cos 2\psi$, and $S_2 = 2|E_+||E_-|\sin 2\psi$. From (44), we can express the ratio $|E_+|/|E_-|$ in terms of $\tan\eta$, from which we compute $S_3 = S_0 \sin 2\eta$ and $2|E_+||E_-| = S_0 \cos 2\eta$. Therefore, we see that the angle 2ψ is the angle from the direction s_1 to the projection of $\vec{s}$ in the $s_1 - s_2$ plane, and 2η is the angle from the $s_1 - s_2$ plane to the vector $\vec{s}$. In other words, we have

$$s_1 = \cos 2\eta \cos 2\psi, \tag{47a}$$

$$s_2 = \cos 2\eta \sin 2\psi, \tag{47b}$$

$$s_3 = \sin 2\eta. \tag{47c}$$

Given the Stokes vector $(s_1, s_2, s_3)^{\mathrm{T}}$, we can find the values of the angles ψ and η by solving the equations:

$$\frac{s_2}{s_1} = \tan 2\psi, \tag{48a}$$

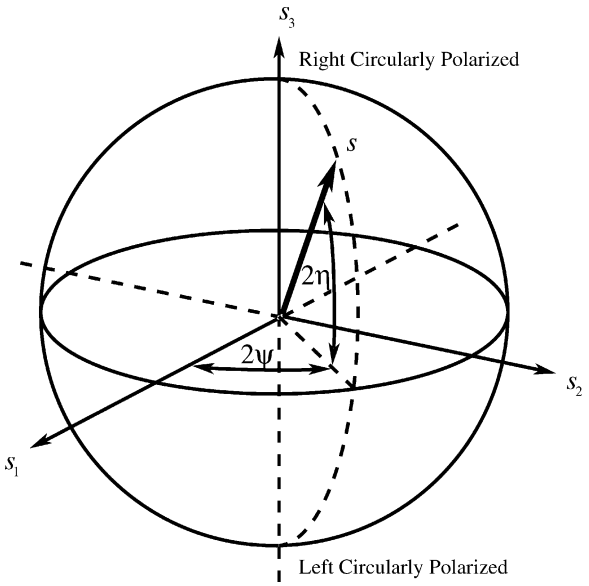

Fig. 9. The Poincaré sphere.

$$s_3 = \sin 2\eta. \tag{48b}$$

Each possible polarization state of a light wave is represented on the Poincaré sphere, with the north and south poles corresponding to right-circularly polarized and left-circularly polarized light, respectively, as drawn in Fig. 9.

To conclude this section, we remark that the concepts explained in this section hold equally well when the constant complex amplitude $\vec{E}$ is replaced by a complex amplitude $\vec{E}(x,t)$ that varies slowly compared with the plane carrier wave $e^{i(kx-\omega t)}$. This is the case in the Λ-configuration of the Maxwell–Bloch equations (1), which we will investigate in more detail in the next section.

4.2. Polarization dynamics of the soliton solutions

In this section, we apply the concepts reviewed in the previous section to the problem at hand, that of bright pulses of polarized light propagating through a two-level medium with a degenerate ground level. For sufficiently long pulses, the two circular polarization components of the light have complex amplitudes $E_\pm(x,t)$ that vary slowly compared to the wavelength and time-period of the light, and satisfy the Λ-configuration Maxwell–Bloch equations (1). In other words, the light inside the optical medium can be represented in the form:

$$\vec{\mathcal{E}}(x,t) = \mathrm{Re}\{[E_+(x,t)\,\vec{\mathbf{e}}_+ + E_-(x,t)\,\vec{\mathbf{e}}_-]\,e^{i(kx-\omega t)}\}$$

with $E_\pm(x,t)$ satisfying equations (1). In what is to follow, we use the polarization ellipse and Stokes' parameters representations introduced in the previous section to study polarization dynamics of light interacting with a Λ-configuration degenerate two-level medium.

We begin with formulas for the general case of the N-soliton solutions. We recall that these solutions are given by formulas (27), obtained from formulas (25), (26) and (24). We substitute these formulas into formulas (45) and

(46) that define the components of the Stokes vector, $\vec{s}$. Consequently, we find the components of the Stokes vector for a general N-soliton solution to be

$$s_1 = \frac{\det C_2^* \det C_3 + \det C_2 \det C_3^*}{|\det C_2|^2 + |\det C_3|^2}, \tag{49a}$$

$$s_2 = \mathrm{i}\frac{\det C_2^* \det C_3 - \det C_2 \det C_3^*}{|\det C_2|^2 + |\det C_3|^2}, \tag{49b}$$

$$s_3 = \frac{|\det C_2|^2 - |\det C_3|^2}{|\det C_2|^2 + |\det C_3|^2}, \tag{49c}$$

where the matrices C_2 and C_3 are defined by formulas (25) and (26). Formulas (49) and (48) now combine to yield the equations:

$$\tan 2\psi = \mathrm{i}\frac{\det C_2^* \det C_3 - \det C_2 \det C_3^*}{\det C_2^* \det C_3 + \det C_2 \det C_3^*}, \tag{50a}$$

$$\sin 2\eta = \frac{|\det C_2|^2 - |\det C_3|^2}{|\det C_2|^2 + |\det C_3|^2} \tag{50b}$$

for the polarization azimuth ψ and the angle of ellipticity η, respectively.

To compute the Stokes vector and the angles ψ and η for the one-soliton solutions (34), we specialize formulas (49) and (50) to the case $N = 1$ with $\lambda_1 = \gamma + \mathrm{i}\mu$, as in Section 3.3, and obtain

$$s_1 = \frac{\cos(\Delta\Omega + \Omega_0)}{\cosh(\Delta\theta + \theta_0)}, \qquad s_2 = \frac{\sin(\Delta\Omega + \Omega_0)}{\cosh(\Delta\theta + \theta_0)}, \qquad s_3 = -\tanh(\Delta\theta + \theta_0). \tag{51}$$

Here, $\Delta\theta$ is given by Eq. (35d) as

$$\Delta\theta = \theta_3 - \theta_2 = \frac{(\mu + \varepsilon)(\alpha_2 - \alpha_3)x}{4[\gamma^2 + (\mu + \varepsilon)^2]},$$

$\Delta\Omega$ is given by

$$\Delta\Omega = \Omega_3 - \Omega_2 = \frac{\gamma(\alpha_2 - \alpha_3)x}{4[\gamma^2 + (\mu + \varepsilon)^2]}$$

with Ω_2 and Ω_3 as defined in Eq. (35), and

$$\theta_0 = \ln\left(\frac{|d_3|}{|d_2|}\right), \qquad \Omega_0 = \arg(d_3^* d_2).$$

Formulae (48) now yield

$$\psi = \frac{\Delta\Omega + \Omega_0}{2}, \qquad \sin 2\eta = -\tanh(\Delta\theta + \theta_0). \tag{52}$$

These results are particularly simple in that they are time-independent. In other words, at each point along the medium, the polarization of the soliton remains unchanged for all times. From formula (52), we first observe that the ellipticity angle either increases or decreases monotonically in x, depending on the sign of the population difference $\alpha_2 - \alpha_3$. If this sign is the opposite of the sign of θ_0, the ellipse passes through linear polarization. Moreover, since the polarization azimuth changes linearly with x, we see that the polarization ellipse rotates at a constant rate while moving along the x-axis. Its sense of rotation is given by the sign of the product $\gamma(\alpha_2 - \alpha_3)$. Formulae (51) show that, on the Poincaré sphere, the polarization of the one-soliton solution traces out a segment

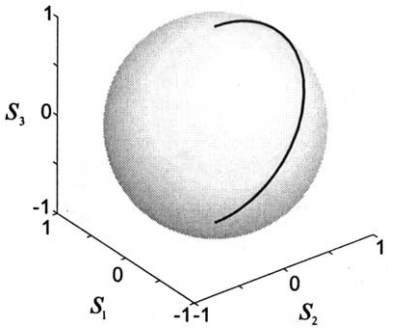

Fig. 10. The Poincaré sphere for the one soliton solution shown in Fig. 3.

of a spiral, connecting the north and south poles of the sphere. Its slope only depends on the ratio $\gamma/(\mu+\varepsilon)$, and not on the population difference $\alpha_2-\alpha_3$. Its sense of rotation is given by the sign of γ. If $\gamma=0$, the spiral segment degenerates into a segment of a great circle. In particular, when the two components $E_+(x,t)$ and $E_-(x,t)$ are real, this circle is the intersection of the Poincaré sphere with the plane $s_2=0$. Along the segment traced out by the one-soliton solution, $s_1>0$ if the soliton is a hump, and $s_1<0$ if the soliton is a dip. In other words, the one-soliton solution cannot traverse a pole but can only approach it, since neither of its components can vanish.

These results stay the same for the one-soliton solution with step-like initial populations, as given by formulas (38). In this case, formulae (51) and (52) remain valid if we use formulas (39) instead of (35) in their definitions. It is interesting to note that, for $x>L$, the point $(s_1(x),s_2(x),s_3(x))$ first exactly retraces the spiral segment it had traced out for $x<L$, but now in the opposite direction. It then continues on and spirals into the pole that signifies the appropriate asymptotic circular polarization. The polarization of the one-soliton solution from Fig. 3 is shown in Fig. 10, where it traces out the zeroth meridian on the Poncaré sphere. Fig. 11 shows the polarization of a complex one-soliton solution, which traces out a spiral. As x increases, approximately the bottom thirds of each the semi-circle and spiral in these two figures, respectively, are traversed twice: first towards the south pole and then back towards the north pole.

Purely real N-soliton solutions still exhibit relatively simple polarization dynamics. In particular, for any fixed time t, the polarizations at all the points inside the medium lie on a segment of the great circle common to the Poincaré sphere and the plane $s_2=0$, and this segment must end at one of the poles. Similarly, at each fixed x, the time evolution of the polarization also traces out a segment of this circle. Such a segment will traverse one of the

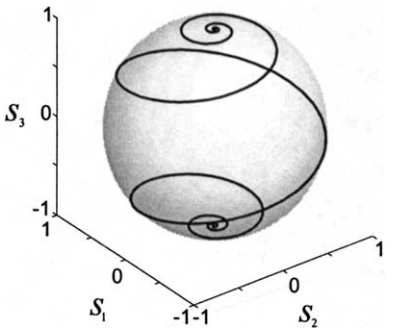

Fig. 11. The Poincaré sphere for the complex one-soliton solution with step-like initial populations, as described by formulas (38), and with parameters $\gamma=2$, $\mu=1/3$, $\varepsilon=1/10$, $L=300$, $\alpha_2=5/6$, $\alpha_3=1/6$, $\beta_2=1/5$, $\beta_3=4/5$, $d_2=d_3=-\mathrm{i}$.

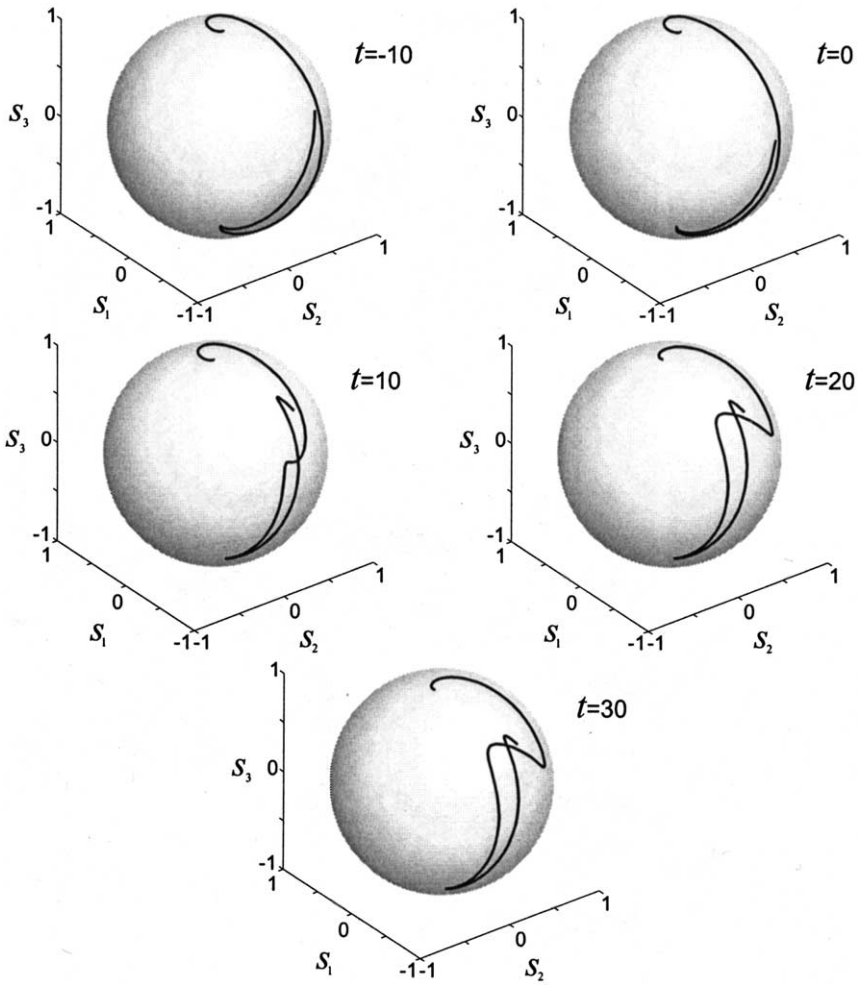

Fig. 12. The Poincaré sphere for the two-soliton solution with step-like initial populations, as described by formulas (38), and parameters $\gamma_1 = 0$, $\gamma_2 = 1/3$, $\mu_j = 1/3$, $\varepsilon = 1/10$, $L = 15$, $\alpha_2 = 5/6$, $\alpha_3 = 1/6$, $\beta_2 = 1/5$, $\beta_3 = 4/5$, $d_{j2} = d_{j3} = -\mathrm{i}$, $j = 1, 2$.

two poles on the Poincaré sphere wherever the appropriate electric field component vanishes. This discussion shows that while the ellipticity angle changes from point to point at any fixed time t and also changes in time at any given point x, the polarization azimuth can take on only two values $\psi = 0$ and $\psi = \pi/2$. In other words, the polarization ellipses at any point of space or time have horizontal and vertical semi-axes. A discontinuous transition between the two values of the azimuth ψ can only occur at points and times when the polarization is circular, in which case ψ loses its meaning altogether.

For general complex N-soliton solutions, the polarization changes from point to point and from moment to moment in a more complicated fashion. An example of a complex two-soliton solution, with step-like initial populations given by formulas (38), is shown in Fig. 12. Each of the curves in the figure is parametrized by x in a fixed time slice, and is composed of two segments joined at the south pole of the Poincaré sphere. The segment joining the two poles is parametrized by $x > L$, while the remaining segment is parametrized by $x < L$. The point $x = L$ is mapped to the south pole. Thus, for x close to L and $x < L$, the light is converted almost entirely to the left-circular

polarization, while the conversion process reverses itself and the light becomes almost completely right-circularly polarized for $x \gg L$.

5. Conclusions

We have described polarization switching of optical pulses injected into a Λ-configuration two-level medium, which is a two-level medium with a degenerate ground level. The precise nature of this switching is determined by the relative population sizes of the two degenerate ground sub-levels. In particular, the switching occurs if the medium is initially prepared in such a way that one of the two degenerate ground sub-levels is consistently more populated than the other. The light switches entirely into the circular polarization that corresponds to the atomic transition between the less populated ground sub-level and the excited level, without losing any of its energy. In this way, asymptotically, far into the medium, the light-medium interaction becomes equivalent to the interaction of light with a non-degenerate two-level medium. We have evaluated the characteristic length associated with the switching of an optical pulse in terms of the spatial widths of its two polarization components shortly after it enters the medium. Finally, we have shown how multiple switchings can be produced and externally controlled by changing the relative population sizes of the degenerate ground sub-levels along the medium.

Acknowledgements

The authors thank D.J. Kaup, A.I. Maimistov, and A. Rahman for comments and discussions. Julie A. Byrne was partly supported by the NSF grants DMS-9502142 and DMS-9510728, and the DOE grant DE-FG02-93ER25154, Ildar R. Gabitov was partly supported by the NSF grant DMS-9510728 and the ARO-FE grant N62649-01-1-0002, Gregor Kovačič was partly supported by the NSF grant DMS-9502142, the DOE grant DE-FG02-93ER25154, the ARO-FE grant N62649-01-1-0002, and an Alfred P. Sloan Research Fellowship. Gregor Kovačič would like to express his gratitude to the faculty and staff of Courant Institute for hosting him during the academic year 2000/2001.

References

[1] C. Cohen-Tannoudji, B. Diu, F. Laloe, Quantum Mechanics, Wiley, New York, 1977.
[2] C.S. Gardner, J.M. Greene, M.D. Kruskal, R.M. Miura, Method for solving the Korteweg–de Vries equation, Phys. Rev. Lett. 19 (1967) 1095–1097.
[3] R.M. Miura, Korteweg–de Vries equation and generalizations. I. A remarkable explicit nonlinear transformation, J. Math. Phys. 9 (1968) 1202–1204.
[4] R.M. Miura, C.S. Gardner, M.D. Kruskal, Korteweg–de Vries equation and generalizations. II. Existence of conservation laws and constants of motion, J. Math. Phys. 9 (1968) 1204–1209.
[5] C.S. Gardner, C.S. Su, The Korteweg–de Vries equation and generalizations. III, J. Math. Phys. 10 (1969) 536–539.
[6] C.S. Gardner, The Korteweg–de Vries equation and generalizations. IV. The Korteweg–de Vries equation as a Hamiltonian system, J. Math. Phys. 12 (1971) 1548–1551.
[7] C.S. Gardner, J.M. Greene, M.D. Kruskal, R.M. Miura, The Korteweg–de Vries equation and generalizations. VI. Methods for exact solution, Comm. Pure Appl. Math. 27 (1974) 97–133.
[8] V.E. Zakharov, A.B. Shabat, Exact theory of two-dimensional self-focusing and one-dimensional self-modulation of waves in nonlinear media, Sov. Phys. JETP 34 (1972) 62–69.
[9] M.J. Ablowitz, D.J. Kaup, A.C. Newell, H. Segur, Nonlinear-evolution equations of physical significance, Phys. Rev. Lett. 31 (1973) 125–127.
[10] M.J. Ablowitz, D.J. Kaup, A.C. Newell, H. Segur, The inverse scattering transform-Fourier analysis for nonlinear problems, Stud. Appl. Math. 53 (1974) 249–315.
[11] M.J. Ablowitz, D.J. Kaup, A.C. Newell, Coherent pulse propagation, a dispersive irreversible phenomenon, J. Math. Phys. 15 (1974) 1852–1858.

[12] G.L. Lamb, Analytical descriptions of ultrashort optical pulse propagation in a resonant medium, Rev. Mod. Phys. 43 (1971) 99–124.
[13] G.L. Lamb, Coherent-optical-pulse propagation as an inverse problem, Phys. Rev. A 9 (1974) 422–430.
[14] D.J. Kaup, Coherent pulse propagation: a comparison of the complete solution with the McCall–Hahn theory and others, Phys. Rev. A 16 (1977) 704–719.
[15] S.M. Zakharov, E.M. Manykin, The inverse scattering formalism in the theory of photon (light) echo, Sov. Phys. JETP 55 (2) (1982) 227–231.
[16] V.E. Zakharov, Propagation of an amplifying pulse in a two-level medium, JETP Lett. 32 (1980) 589–593.
[17] S.V. Manakov, Propagation of ultrashort optical pulse in two level laser amplifier, Sov. Phys. JETP 56 (1) (1982) 37–44.
[18] S.V. Manakov, V.Yu. Novokshonov, Complete asymptotic representation of an electromagnetic pulse in a long two-level amplifier, Theoret. Mater. Phys. 69 (1) (1986) 40–54.
[19] I.R. Gabitov, A.V. Mikhailov, V.E. Zakharov, Superfluorescence pulse shape, JETP Lett. 37 (5) (1983) 279–282.
[20] I.R. Gabitov, A.V. Mikhailov, V.E. Zakharov, Nonlinear theory of superflourescence, Sov. Phys. JETP 59 (4) (1984) 703–709.
[21] I.R. Gabitov, A.V. Mikhailov, V.E. Zakharov, Maxwell–Bloch equation and the inverse scattering method, Theoret. Mater. Phys. 63 (1) (1985) 328–343.
[22] A.M. Basharov, A.I. Maimistov, Self-induced transparency when the resonance energy levels are degenerate, Sov. Phys. JETP 60 (1984) 913–919.
[23] A.I. Maimistov, Rigorous theory of self-induced transparency in the case of a double resonance in a three-level medium, Sov. J. Quant. Electron. 14 (1984) 385–389.
[24] A.I. Maimistov, New examples of exactly solvable problems in nonlinear optics, Opt. Spetrosc. (USSR) 57 (1985) 340–341.
[25] A.I. Maimistov, Y.M. Sklyarov, Coherent interaction of light pulses with a three-level medium, Opt. Spectrosc. 59 (4) (1985) 459–461.
[26] A.M. Basharov, A.I. Maimistov, Polarized solitons in three-level medium, Sov. Phys. JETP 67 (1988) 2426–2433.
[27] L.A. Bolshov, V.V. Likhanskii, M.I. Persiantsev, Contribution to the theory of coherent interaction of light pulses with resonant multilevel media, Sov. Phys. JETP 57 (1983) 524–528.
[28] L.A. Bolshov, V.V. Likhanskii, Coherent interaction of radiation pulses with resonant multilevel media (review), Sov. J. Quant. Electron. 15 (1985) 889–904.
[29] L.A. Bolshov, N.N. Elkin, V.V. Likhanskii, M.I. Persiantsev, Coherent amplification of radiation under forward resonant stimulated Raman scattering, Sov. Phys. JETP 61 (1985) 27–33.
[30] L.A. Bolshov, N.N. Elkin, V.V. Likhanskii, M.I. Persiantsev, Theory of coherent frequency conversion via ultrashort pulses in resonant media, Sov. Phys. JETP 67 (10) (1988) 2013–2017.
[31] I.R. Gabitov, A.V. Mikhailov, Superfluorescence under atomic level degeneration, in: V.G. Bar'Yakhtar, V.M. Chernousenko (Eds.), Plasma Theory and Nonlinear and Turbulent Processes in Physics, World Scientific, Singapore, 1988, pp. 779–787.
[32] H. Steudel, N-soliton solutions to degenerate self-induced transparency, J. Mod. Opt. 35 (1988) 693–702.
[33] S.B. Leble, N.V. Ustinov, On soliton and periodic solutions of Maxwell–Bloch system for two-level medium with degeneracy, Solitons Fractals 11 (2000) 1763–1772.
[34] A. Rahman, Optical pulse propagation in inhomogeneously broadened V-type three-level media, Ph.D. Thesis, University of Rochester, 1999.
[35] J.A. Byrne, Mathematical modeling of multiresonance problems in nonlinear optics, Ph.D. Thesis, Rensselaer Polytechnic Institute, 2000.
[36] D.J. Kaup, The inverse-scattering transform for three-level coherent pulse propagation, in: Presentation at the Conference on Soliton Equations: Applications and Theory, University of Colorado at Colorado Springs, 2001.
[37] A.M. Basharov, S.O. Elyutin, A.I. Maimistov, Y.M. Sklyarov, Present state of self-induced transparency theory, Phys. Rep. 191 (1990) 1–108.
[38] S.V. Manakov, On the theory of two-dimensional stationary self-focusing of electromagnetic waves, Sov. Phys. JETP 38 (2) (1974) 248–253.
[39] M.J. Ablowitz, H. Segur, Solitons and the Inverse Scattering Transform, SIAM, Philadelphia, PA, 1981.
[40] J.D. Jackson, Classical Electrodynamics, 2nd ed., Wiley, New York, 1975.
[41] M. Born, E. Wolf, Principles of Optics; Electromagnetic Theory of Propagation, Interference, and Diffraction of Light, Pergamon Press, Oxford, 1975.